Paper 04S-023

Active Control for Turbulent Premixed Flame Simulations

J. B. Bell, M. S. Day, J. F. Grcar and M. J. Lijewski

Lawrence Berkeley National Laboratory
Mail Stop 50A-1148
One Cyclotron Road
Berkeley, CA 94720-8142 USA

e-mail contact: MSDay@lbl.gov

Abstract

Many turbulent premixed flames of practical interest are statistically stationary. They occur in combustors that have anchoring mechanisms to prevent blow-off and flashback. The stabilization devices often introduce a level of geometric complexity that is prohibitive for detailed computational studies of turbulent flame dynamics. As a result, typical detailed simulations are performed in simplified model configurations such as decaying isotropic turbulence or inflowing turbulence. In these configurations, the turbulence seen by the flame either decays or, in the latter case, increases as the flame accelerates toward the turbulent inflow. This limits the duration of the eddy evolutions experienced by the flame at a given level of turbulent intensity, so that statistically valid observations cannot be made. In this paper, we apply a feedback control to computationally stabilize an otherwise unstable turbulent premixed flame in two dimensions. For the simulations, we specify turbulent inflow conditions and dynamically adjust the integrated fueling rate to control the mean location of the flame in the domain. We outline the numerical procedure, and illustrate the behavior of the control algorithm. We use the simulations to study the propagation and the local chemical variability of turbulent flame chemistry.

1 Introduction

Premixed turbulent flames are of considerable practical importance and remain an important subject for research in the combustion community. Experimentalists have studied a variety of flame configurations which can be categorized by the flame stabilization mechanism. For example, the Twenty-Nineth Combustion Symposium includes studies by Sattler et al. [1] of a turbulent V-flame, Shepherd et al. [2] of a swirl-stabilized flame, Most et al. [3] of a bluff-body stabilized flame, and Chen et al. [4] of Bunsen and stagnation flames. These stabilization mechanims are necessary to control the flame location so that data can be collected from a statistically stationary flame. Each of these stabilization mechanisms has advantages and disadvantages. Bluff-body stabilized flame, V-flames and bunsen flames are fluid-mechanically fairly simple but these is substantial flow tangential to the flame and the flame encounters different different levels of turbulence further from the burner nozzle. The low-swirl geometry produces a nearly flat flame but the fluid mechanics of the flame is quite complex. Stagnation plate flames are geometrically and fluid mechanically simple but the flame experiences a substantial mean strain.

For the most part, computational studies of premixed flames that include detailed chemistry and transport and resolve the relevant fluid-mechanical scales have not included any of these stabilization mechanisms. (For an exception, see Bell et al. [5] which models a 3D turbulent V-flame.) The computational demands of these types of simulations combined with the specialized numerical algorithms typically used for direct numerical simulations make including physical stabilization mechanisms nearly impossible. Consequently, most DNS studies of turbulent flame dynamics have not included any flame stabilization mechanism. Typically, numerical simulations of turbulent premixed flames initialize a laminar premixed flame in the computational domain and specify an inflow mean flow boundary condition with the superimposed turbulent perturbations which are then allowed to propagate up to the flame.

There is an extensive literature on computational studies of premixed turbulent flames in two dimensions, both with simplified and detailed chemistry. Examples germane to the type of configuration we wish to consider include Baum et al. [6] who studied turbulent flame interactions for detailed hydrogen chemistry, and Haworth et al. [7] who examined the effect of inhomogeneous reactants for propane–air flames using detailed propane chemistry.

Three-dimensional studies in which incoming turbulence interacts with a laminar flame were first studied by Trouve and Poinsot [8] and by Zhang and Rutland [9] for simplified chemistry. More recently Tanahashi et al. [10, 11] have performed simulations of this type for turbulent, premixed hydrogen flames with detailed hydrogen chemistry. Bell et al. [12] performed a similar study for a turbulent methane flame.

Although the types of computational studies described above provide a great deal of useful information about the flame dynamics, the flames they consider are inherently unstable. If the flame begins to propagate faster than the specified inflow velocity, the flame encounters stronger turbulence which increases its speed. Similarly, a speed slower than the inflow velocity leads to flame deceleration. As a result, the flame is not statistically stationary and will often propagate to either the domain inflow or outflow boundary. In the present paper, we apply a control algorithm that stabilizes these types of flames on the computational grid using a simple feedback mechanism. As a result, the flames become statistically stationary enabling a detailed characterization of the flame at statistically fixed conditions. In the next section, we briefly describe the basic simulation methodology and describe the feedback control procedure. We then demonstrate the ability of the algorithm to stabilize premixed methane flames in two dimensions. We then use the stabilized flames to compute localized flame speed statistics and estimate Markstein lengths for two different stoichiometries. Finally, we examine the role of chemistry in local flame speed variability.

2 Computational Model

The simulations presented here are based on a low Mach number formulation of the reacting flow equations. The methodology treats the fluid as a mixture of perfect gases. We use a mixture-averaged model for differential species diffusion and ignore Soret and Dufour effects. Radiative heat transfer is modeled using an optically thin approximation. The chemical kinetics are modeled using the GRI-Mech 3.0 methane mechanism [13] with 53 species and 325 fundamental reactions. Our basic discretization algorithm combines a symmetric operator-split coupling of chemistry and diffusion processes with a density-weighted approximate projection method for incorporating the velocity divergence constraint arising from the low Mach number formulation. This basic integration scheme is embedded in a parallel adaptive mesh refinement algorithm. Our approach to adaptive refinement is based on a block-structured hierarchical grid system composed of nested rectangular grid patches. The adaptive algorithm is second-order accurate in space and time, and discretely conserves species mass and enthalpy. The reader is referred to [14] for details of the low Mach number model and its numerical implementation and to [12] for previous applications of this methodology to the simulation of premixed turbulent flames.

The basic flow configuration we consider initializes a flat laminar flame in the domain oriented so the flame is propagating downward. Inflow is specified at the bottom of the domain and outflow is specified at the top. The other boundaries are periodic. At the inflow face we specify both a mean inflow velocity and turbulent fluctuations that are superimposed on the mean inflow. The objective here is to use a simple feedback control to automatically adjust the inflow velocity to maintain the mean location of the flame in the domain. For the purposes of controlling the flame, the mean flame location, x can be computed by integrating the mass of fuel in the domain and normalizing by the inflow fuel density $\times$ the inflow area. We do not know the turbulent flame speed, s; it must be estimated as part of the control process. In practice, the flame speed will not, in fact, be constant. There will be some degree of fluctuations in the flame speed. Although these variations in speed are a deterministic property of the evolving flame geometry, for the purposes of controlling the flame location we will view these variations as noise in the flame speed.

With these definitions, the flame location satisfies the stochastic differential equation

$$dx = (v_{in}(t) - s)dt + d\omega$$

where v_{in} is the mean inflow velocity and $d\omega$ represents fluctuations in the turbulent flame speed. The control problem can then be stated as: Given $x(0) = \alpha$, estimate s and find $v_{in}(t)$ so that $x(t) \rightarrow \beta$ where α and β are the initial and target flame locations, respectively. Because the control velocity $v_{in}(t)$ determines the boundary condition for the low Mach number solver, we need to impose additional constraints on the profile. In particular, we will enforce that the profile is piecewise linear and limited such that the inflow velocity cannot change dramatically during a time step. These smoothness criteria on the control constrain how rapidly the v_{in} can respond to changes in x and to noise. Consequently, we need to introduce a time scale τ which is the target lag for reaching the control state. In particular, from time t_0 we want to estimate v so that x reaches β at $t_0 + \tau$. We assume that τ is sufficiently large that the noise $d\omega$ has mean zero over the interval $[t, t + \tau]$. Then, given $x(t_0)$ and $v_{in}(t_0)$, we can integrate the ODE to obtain

$$\beta = x(t_0 + \tau) = x(t_0) + \int_{t_0}^{t_0+\tau} v_{in}(t_0) + (t - t_0)\Delta v - s_{est}dt$$

Given an estimate for the turbulent flame speed s_{est} we can solve the above equation for Δv, the slope of the inflow velocity profile. For the purposes of computing this integral, we estimate s_{est}

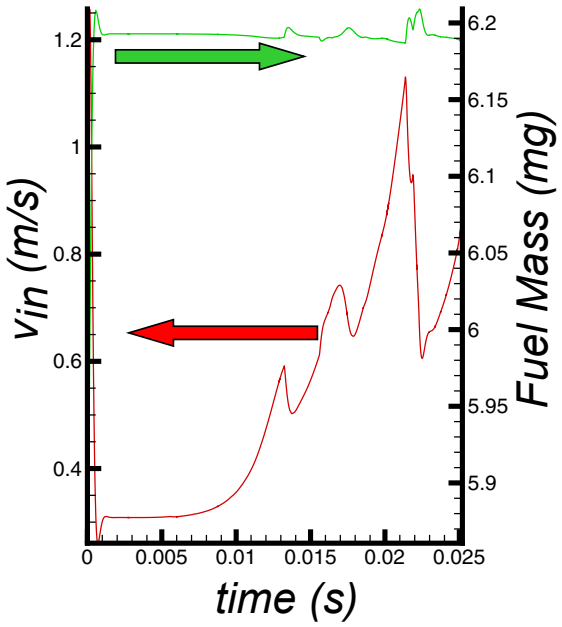

Figure 1: *Performance of control algorithm for* $\phi = 1.0$ *case.*

from the change in fuel mass in the domain during the previous time step. If the predicted Δv produces too large a change in velocity, we reduce its magnitude as required. From computational experiments, we have found that $\tau = O(10)\Delta t$ combined with a restriction that we not change the velocity by more than 5% during a time step results in fairly reponsive control of the flame location without causing any difficulty for the flow solver. Also, we find the flow solver to be more robust if we minimize the outflow at the inflow face by preventing negative values of v_{in}, choosing rather to let the flame burn upstream with $v_{in} = 0$, if necessary for control.

We apply the control methodology to the simulation of premixed methane flames as they interact with perturbations in the velocity field of an inflowing fuel stream. A set of three premixed flames are chosen to highlight variations observed the the flame response to flowfield strain and flame surface curvature. The three cases have stoichiometries, $\phi = 0.55,\ 0.75,\ 1.0$, and thermal thicknesses, $\delta_L^T = 1313$, 584 and 433 μm, respectively. The computational domain in all three cases is periodic in the x-direction with inflow on the low y face and outflow at the high y face, and has dimensions $46\delta_L^T \times 92\delta_L^T$. Fluctuations in the inflow stream were generated with an effective integral scale length approximately XX times the thermal width so that the inflow face accomodates approximately XX mean-sized eddies. The fluctuation intensity, u', of the inflowing turbulence is isotropic and equal to XXs_L, where s_L is the propagation speed of the corresponding flat laminar flame, as computed using the PREMIX [15] code. Adaptive mesh refinement was used in all the simulations to maintain approximately 22 uniform grid cells across the thermal width of the flames throughout their evolution. Dynamic refinement for these simulations were based on the magnitude of vorticity and on a flame marker, HCO. In each case, we evolved the the simulations until the flame height stabilized, and then began accumulating snapshots for analysis.

As an example of the performance of the control iterations, we show in Figure 1 the flame location and control velocity for the $\phi = 1$ case as a function of simulation time. Here, we initialized the solution with a one-dimensional premixed flame solution from PREMIX, setting the flame position lower than a target height, which we arbitrarily set to one quarter the domain height.

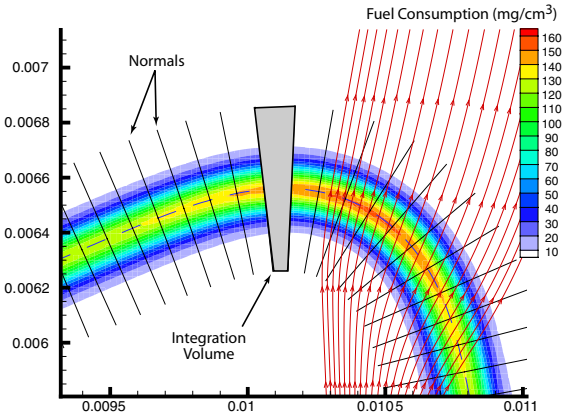

Figure 2: *Typical construction of flame normals and integration volumes, based here on phi* $= 1.0$ *solution at* $t = 16$ *ms. Background colored by local fuel consumption rate. The dotted blue line represents* $T = T_{Q_{max}} = 1692K$*, and the arrows follow the instantaneous flow velocity streamlines.*

The initial transient indicates that the control quickly increases the fueling rate to shift the flame upward. As the target height is approached, a small overshoot is observed as the inflow velocity is adjusted automatically to zero over a finite time. After the flame burns upstream to the proper location, the control settles into a value near 30 cm/s as the inflowing turbulence propagates toward the flame surface. At approximately 8 ms, the flame surface area begins to grow, increasing the effective flame area and integrated fuel consumption. The control procedure adapts the inflow rate in response to maintain a nearly constant fuel inventory in the domain, showing only modest perturbations with dramatic changes in fuel burning rates. The large transients in fuel consumption correspond to flame topology changes such as localized necking and pinching off of flame fragments.

3 Analysis

For the initial analysis of the results, we explore the relationship between aggregate flame speed, s_T, based on fuel consumption, and the flame area resulting from wrinkling due to the inflow fluctuations. We compute the flame area, a_T, by measuring the length in two-dimensions of the temperature contour corresponding to that of maximum heat release in a flat, steady premixed flame of the same stoichiometry, ie. $T \equiv T_{Q_{max}}$. In Figure XX, we plot s_T versus $s_L a_T / a_L$ where s_L, a_L are the speed and length of the corresponding flat steady flame. To a very good approximation, the fuel consumption rate in the domain scales with the overall area of the flame in all three case.

To refine the analysis of flame speed we look at its variation along the flame surface, defined in terms of the localized fuel consumption. In particular, we construct equi-spaced normals to the flame along the temperature contour, $T = T_{Q_{max}}$, and use them to define a collection of wedge-shaped regions that cover the region where fuel is consumed. A typical example of a set of such normals, and the resulting wedge-shaped volumes is depicted in Figure 2. A local flame speed may then be defined as the integral of the fuel consumption over a wedge divided by the length of the flame contour contained in the wedge, and scaled by the mass flux of fuel into the domain. In Figure 3, we show the local flame speed plotted along the flame surface as a function of arc-length along the flame contour for three case at representative snapshots in time. Here, the curve indicating the flame location is colored by the local tangential strain rate, $\mathcal{S} = \hat{t} \cdot \nabla U \cdot \hat{t}$, normalized

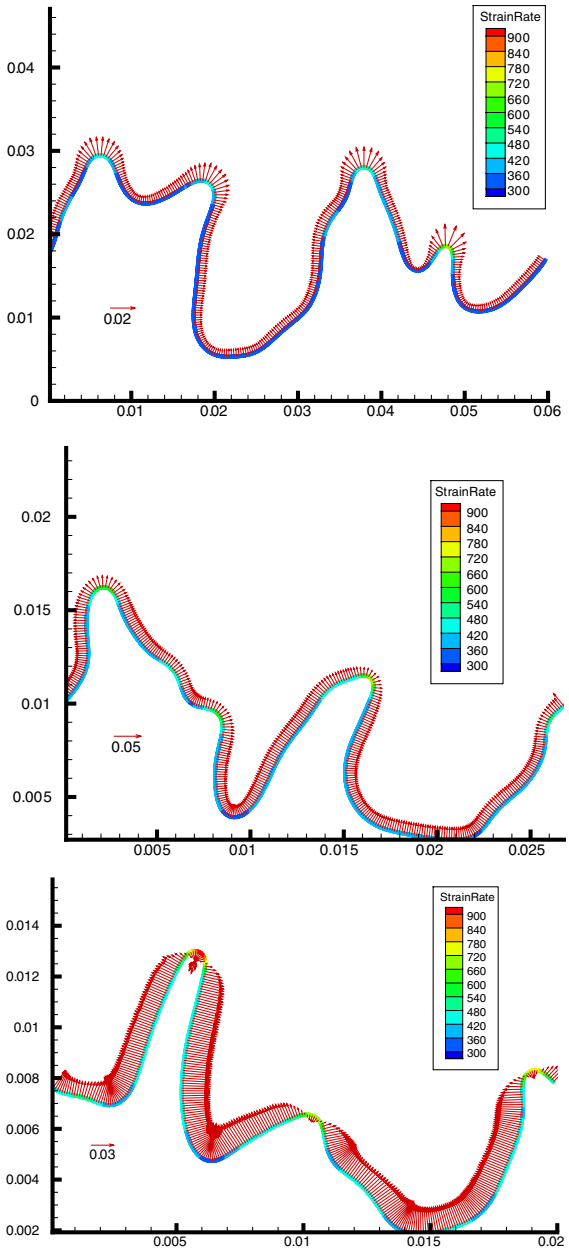

Figure 3: *Local burning speeds along representative flame surfaces for $\phi = 0.55$ (top), $\phi = 0.75$ (middle) and $\phi = 1.0$ (bottom). Flame surface is colored by the normalized tangential strain, and burning speeds are plotted (in m/s) with repect to the laminar flame speed, s_L, and directed normal to the flame.*

by s_L/δ_L^T, and $\hat{t}$ is a unit tangent along the flame surface. The variation in the local flame speed relative to the laminar burning velocity is depicted as a vector locally normal to the flame, and scaled such that it points into the unburnt region if the local speed is larger than the laminar speed, and into the burnt region if it is smaller. The correlation of the flame speed with flame curvature is apparent.

From wrinkled flame theory, (cf. Peters [16]), we expect the local flame speed to correlate with

curvature κ and $\mathcal{S}$ according to the relationship

$$s_{loc} = s_L(1 - \kappa\mathcal{L}) - \mathcal{S}\mathcal{L}$$

where $\mathcal{L}$ is the Markstein length. At the time of presentation of this work, we will show scatter plots of s_{loc} and $s_L(1-\kappa) - \mathcal{S}$ for $\phi = 0.55,\ 0.75\ 1.0$. In these plots, the slope of a linear fit defines the Markstein length, and the deviation from the fit shows the degree to which the theory matches the observed local speed over the observed range of curvature and strain rates. As a further characterization of the deviation of the observed data from theory, we will present scatter plots of s_{loc} versus κ and $\mathcal{S}$ independently.

We will present estimates of Markstein lengths for the three equivalence ratios The magnitude of Markstein length for the $\phi = 0.75$ flame is much smaller than for either of the other flames, while those the of the remaining case are of opposite sign. This indicates that the $\phi = 0.75$ case is near a transition in thermodiffusional stability.

To quantify the role of detailed chemistry and transport on the variation in Markstein length, we first define local equivalent atomic concentrations. In particular, we define

$$\beta_C = \frac{2N_C}{2N_C + N_H/2 + N_O} \quad \beta_H = \frac{N_H/2}{2N_C + N_H/2 + N_O} \quad \beta_O = \frac{N_O}{2N_C + N_H/2 + N_O}$$

where $N_X,\ X = C, H, O$ is the total number of atoms of element X per unit volume at each point in the domain. For a stoichiometric mixture of methane and oxygen, $\beta_C = \beta_H = 0.25$ and $\beta_O = 0.5$. We will present plots of the β's over the two-dimensional domain for all three stoichiometries. The figures will show that relative to the inflow mixture, the region in front of the flame is slightly leaner than the inflow mixture. More importantly, the region on the unburnt side of the flame is rich in hydrogen and the burnt side is rich in carbon relative to the inflow mixture. The dominant reason for this behavior is the high diffusivity of H_2. The H_2 molecules are formed within the flame and are able to diffusive forward into the unburnt region. In regions of negative curvature, this effect is enhanced while it is reduced in regions of positive curvature. Convective transort also plays a role in enriching the H concentration of regions of negative curvature. Increasing the available H_2 increases the local burning intensity and plays a key role in increasing the local burning speed. Comparison of the data for the stoichiometric flame and the lean flame shows that the hydrogen enrichment in front of the flame and the subsequent focusing of hydrogen in regions of negative curvature are dramatically reduced. This occurs because H_2 reacts more quickly in the more oxygen rich environment. The variation in Markstein number with equivalence ratio for methane combustion is intimately linked to the availability and diffusive behavior of H_2.

4 Conclusions

We have introduced a new computational tool based on applying a feedback mechanism to control and stabilize a turbulent flame in a simple two dimension geometry without introduce either a geometric stabilization mechanism such as a flow obstruction of a stagnation plate. We have used this tool to study the behavior of premixed turbulent methane flames in two dimensions. For these simulations we are examining both the global flame behavior and the dependence of the local flame speed on flame curvature and flow field straining.

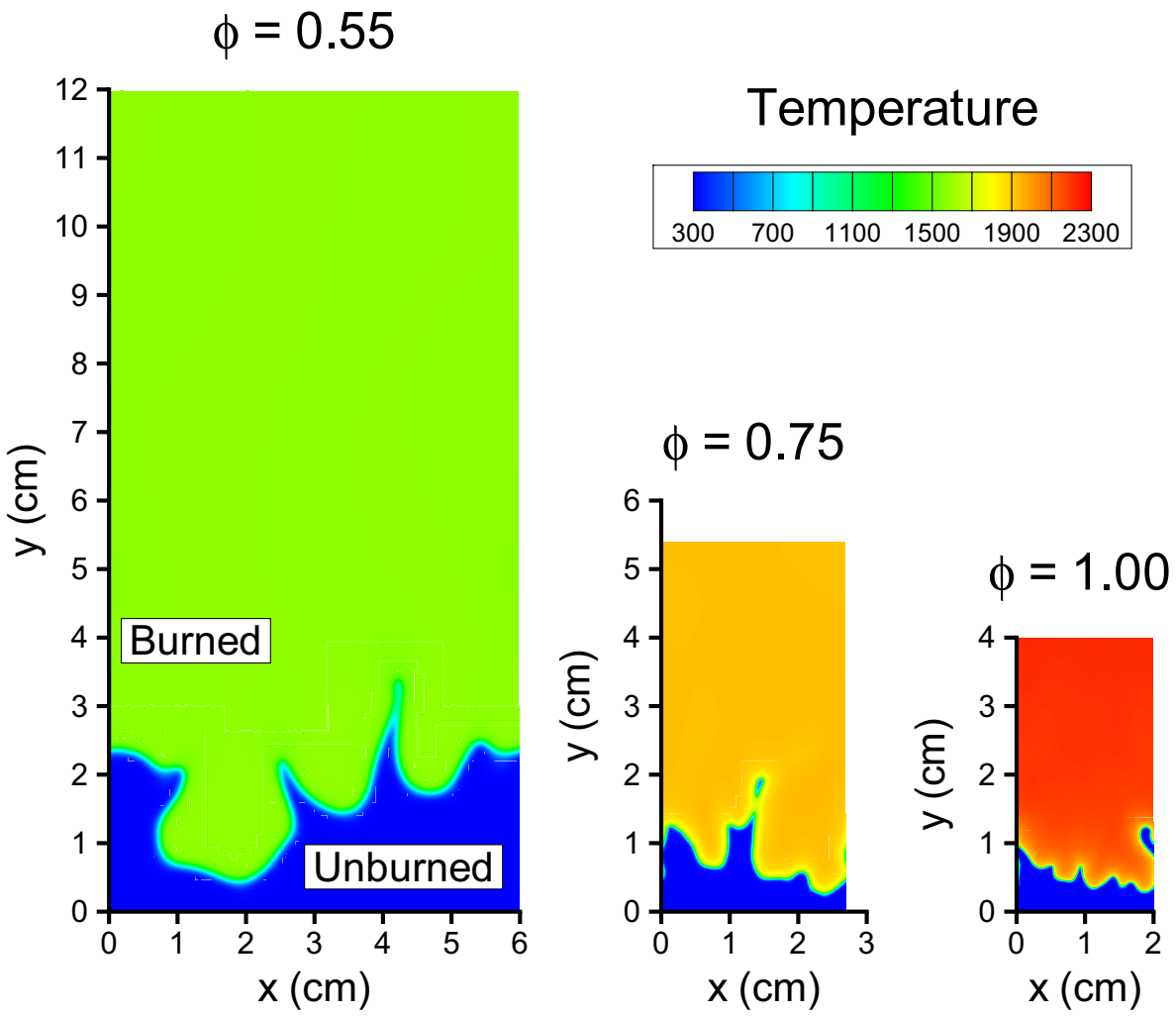

Figure 4: *Temperture in the three flames.*

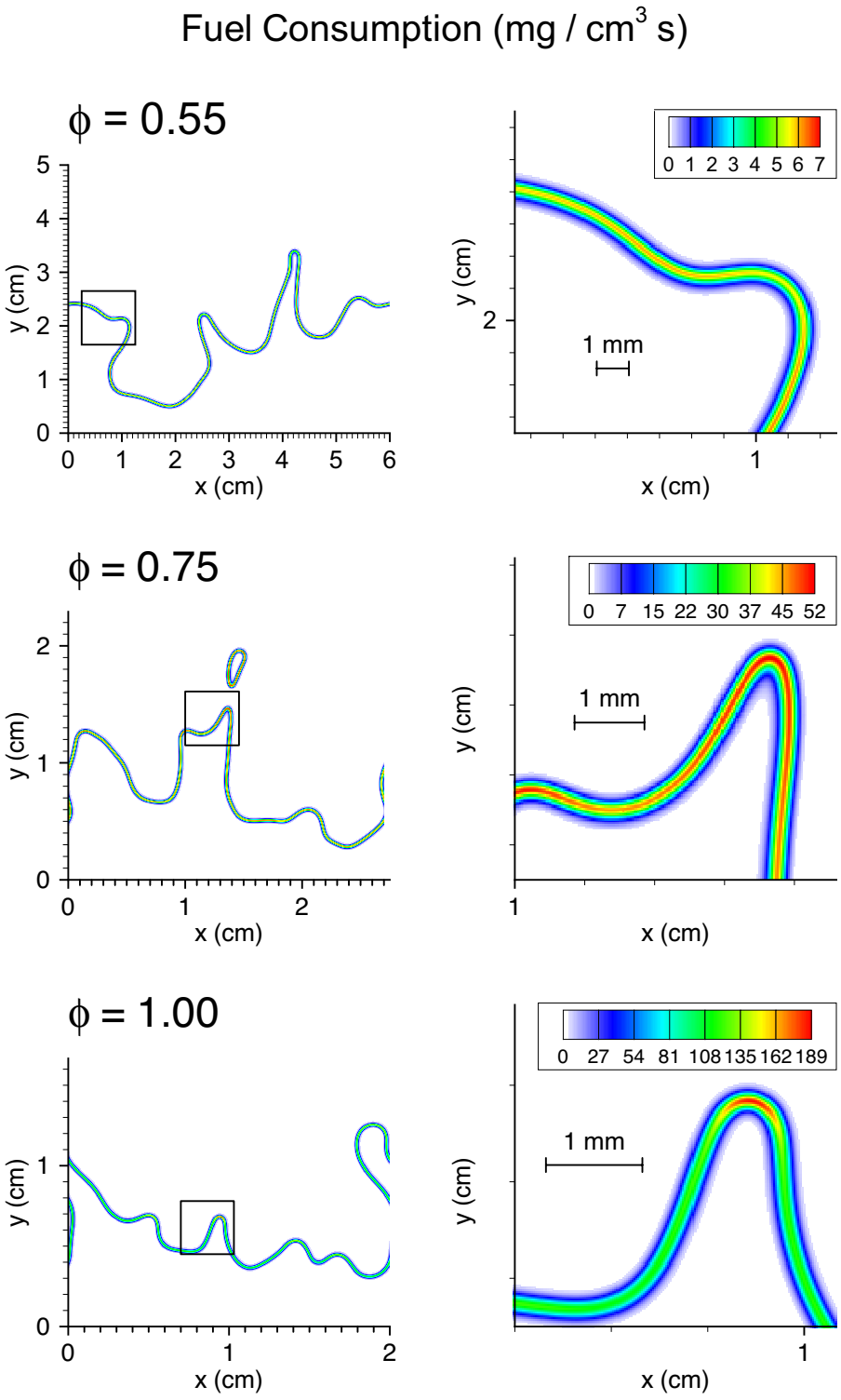

Figure 5: *Fuel consumption in the three flames.*

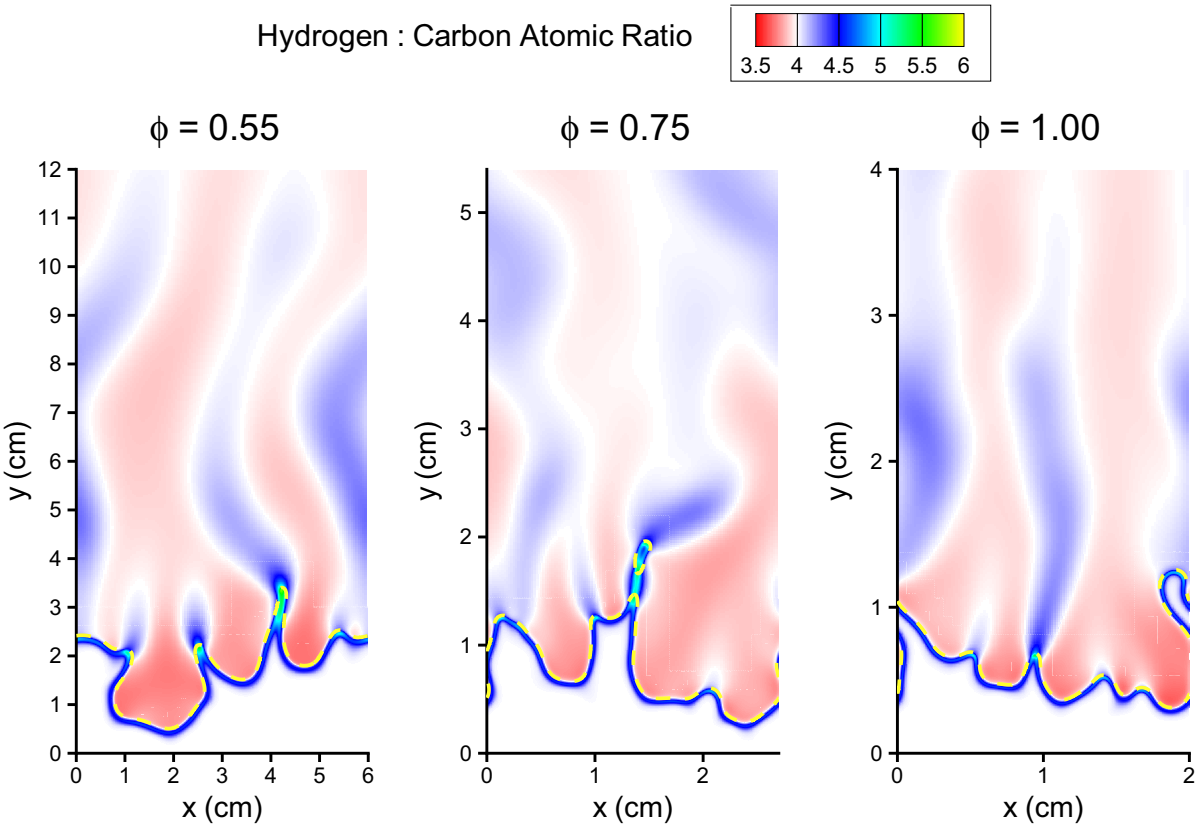

Figure 6: *Ratio of hydrogen to carbon atoms in the three flames.*

References

[1] Sattler, S. S., Knaus, D. A., and Gouldin, F. C., *Proc. Combust. Inst.*, 29:1785–1795 (2002).

[2] Shepherd, I. G., Cheng, R. K., Plessing, T., Kortschik, C., and Peters, N., *Proc. Combust. Inst.*, 29:1833–1840 (2002).

[3] Most, D., Dinkelacker, F., and Leipertz, A., *Proc. Combust. Inst.*, 29:1801–1806 (2002).

[4] Chen, Y.-C., Kalt, P. A. M., Bilger, R. W., and Swaminathan, N., *Proc. Combust. Inst.*, pp. 1863–1871 (2002).

[5] Bell, J. B., Day, M. S., Shepherd, I. G., Johnson, M., Cheng, R. K., Beckner, V. E., Lijewski, M. J., and Grcar, J. F., "Numerical simulation of a laboratory-scale turbulent V-flame," Technical Report No. LBNL-54198, Submitted for publication.

[6] Baum, M., Poinsot, T. J., Haworth, D. C., and Darabiha, N., *J. Fluid Mech.*, 281:1–32 (1994).

[7] Haworth, D. C., Blint, R. J., Cuenot, B., and Poinsot, T. J., *Combust. Flame*, 121:395–417 (2000).

[8] Trouve, A. and Poinsot, T. J., *J. Fluid Mech.*, 278:1–31 (1994).

[9] Zhang, S. and Rutland, C. J., *Combust. Flame*, 102:447–461 (1995).

[10] Tanahashi, M., Fujimura, M., and Miyauchi, T., *Proc. Combust. Inst.*, 28:529–535 (2000).

[11] Tanahasi, M., Nada, Y., Ito, Y., and Miyauchi, T., *Proc. Combust. Inst.*, 29:2041–2049 (2002).

[12] Bell, J. B., Day, M. S., and Grcar, J. F., *Proc. Combust. Inst.*, 29:1987–1993 (2002).

[13] Frenklach, M., Wang, H., Goldenberg, M., Smith, G. P., Golden, D. M., Bowman, C. T., Hanson, R. K., Gardiner, W. C., and Lissianski, V., "GRI-Mech—an optimized detailed chemical reaction mechanism for methane combustion," Gas Research Institute Technical Report No. GRI-95/0058, http://www.me.berkeley.edu/gri_mech/.

[14] Day, M. S. and Bell, J. B., *Combust. Theory Modelling*, 4:535–556 (2000).

[15] Kee, R. J., Grcar, J. F., Smooke, M. D., and Miller, J. A., "A fortran program for modeling steady, laminar, one-dimensional premixed flames," Sandia National Laboratories Report No. SAND85-8240.

[16] Peters, N., *Turbulent Combustion* , Cambridge University Press, Cambridge, UK, 2000.